EasyChair Preprint

№ 9796

Relating Permeability to 3D Crack Topography to Evaluate the Healing Efficiency in Carcked Reactive Powder Concrete

Sailong Hou, Caijun Shi, Kai Li and Xiang Hu

February 28, 2023

The 16th International Congress on the Chemistry of Cement 2023 (ICCC2023)
"Further Reduction of CO_2 -Emissions and Circularity in the Cement and Concrete Industry"
September 18–22, 2023, Bangkok, Thailand

Relating permeability to 3D crack topography to evaluate the healing efficiency in cracked reactive powder concrete

S. Hou [1,2,3,a], C. Shi[1,2,3,b*], K. Li[1,2,3,c] and X. Hu[1,2,3,d]

[1] *College of Civil Engineering, Hunan University, Changsha, PR China*

[2] *Key Laboratory for Green & Advanced Civil Engineering Materials and Application Technologies of Hunan Province, Changsha, PR China*

[3] *International Innovation Center for Green & Advanced Civil Engineering Materials of Hunan Province, Changsha, PR China*

Email: [a]*civilhsl@hnu.edu.cn*
Email: [b]*cshi@hnu.edu.cn*
Email: [c]*likai@hnu.edu.cn*
Email: [d]*xianghu@hnu.edu.cn*

ABSTRACT

The self-healing effects of concrete alter the 3D crack topography by accumulating newly formed products, which changes the water flow behavior and results in a reduction in water permeability. This study utilized laser scanner and water permeability tests to establish a feedback mathematical model that quantifies the relationship between 3D crack topography and the intrinsic permeability of reactive powder concrete (RPC). The model is expected to predict the effect of healing product accumulation on crack topography. The intrinsic permeability was characterized by Darcy's law, and the 3D crack topography was reconstructed using point-cloud matching technology. Cracked RPCs with various widths were immersed in water for 120 days, and it was found that water permeability reduction can be attributed to local crack width reduction, which may even form an obstacle with zero width. When all interconnected paths are cut by newly produced precipitates, water permeability decreases to zero, even though many voids may remain in the crack topography. After healing, variations in crack surface roughness are observed, but the mean crack widths of all specimens decrease.

KEYWORDS: *Self-healing concrete; Crack topography; Water permeability test; Feedback model; Healing efficiency*

1. Introduction

Self-healing concretes have become a popular topic of research in recent decades, owing to their environmentally friendly and sustainable properties. The process of healing in concrete is a complex set of physical and chemical reactions, as previously noted in studies conducted by (Hou et al (2022), Zhang et al (2020)). While the "healing phenomenon" may be visually observed when cracks are sealed by white crystals, this does not necessarily indicate that the concrete's functional capacity has been fully restored, as noted by (Suleiman and Nehdi (2018)). The key to understanding the self-healing properties of concrete lies in its mechanical capacity recovery and durability improvement, which can be attributed to the sealing of multiscale cracks by healing products (Yoo et al (2020), Xue et al (2022)). Therefore, it is essential to study the changes in 3D crack topography that occur as healing actions enhance the functions of damaged concretes. Water flow behaviors are particularly sensitive to crack geometry, including crack width and obstacles, as well as pressure gradient (∇P) (Xiong et al (2018), Hou et al (2023)). In the water permeability test of self-healing concrete, the controlled ∇P is always considered reasonable to deduce its hydraulic properties, as demonstrated by (Akhavan et al (2012)). The hydraulic properties of concrete, such as water

permeability, are closely associated with its durability. Thus, when healing products alter the crack topography of concrete, decrease the crack width, and form obstacles on interconnected flow paths, the permeability can be significantly reduced, as observed by (Wu et al (2018), Mountassir et al (2014), Lepech and Li (2009)). In their study, (Fan and Li (2022)) attempted to explain the mechanisms of the healing process along the crack depth in physicochemical actions using modeling and experiments. They found that the distribution of healing products in the crack topography was uneven, a finding that has also been reported by (Suleiman and Nehdi (2018), Huang et al (2016), Hou et al (2022)). However, more research is needed to quantify and illustrate the effects of self-healing on the inner crack topography.

This study aims to establish a feedback model that links permeability decrement and 3D crack topography alternation, providing further insight into the intrinsic healing mechanisms of concrete. The reactive powder concrete (RPC) was first digitized to record the pre-conditioning crack surface morphology. The crack width of the specimen was then artificially designed 123.45 μm. Next, the permeability of the tested specimen was determined, after which they were subjected to 120 days of wet/dry cycles while immersed in water. After the specimen was healed, the permeability were measured, and the healed surface morphologies were recorded again. The reconstruction of crack topography followed the methodology established in previous studies (Hou et al (2023)), allowing us to deduce the variability of pre-conditioning and after-conditioning specimens. Through this process, we aim to establish a feedback model between water permeability and 3D crack topography, providing insights into the mechanisms of self-healing in concrete.

2. Experimental program

2.1 Raw material and specimen preparation

Portland cement Type I 42.5 (PI 42.5), silica fume (SF) and ground granulated blast-furnace slag (GGBS) are used as raw materials for specimen preparation. Their physical and chemical properties are given in Table 1. Silica sand (SS) (0.058-0.25 mm), fine river sand (FS) (0.6-1.18 mm) and coarse river sand (CS) (1.18-2.36 mm) are utilized as aggregates. The mass ratio of sand to cement (s/c) and water to cement (w/c) are set as 1 and 0.2, respectively. Tap water and high range water reducer are employed and the mixture proportion adopted in this work is shown in Table 2.

Table 1. Properties of PI 42.5, SF and GGBS

Components/Properties	PI 42.5	SF	GGBS
SiO_2	22.87%	95.4%	35.02%
Al_2O_3	4.47%	-	14.84%
Fe_2O_3	3.48%	0.54%	1.2%
CaO	64.05%	1.65%	37.01%
MgO	2.46%	0.26%	0.2%
SO_3	2.44%	-	1.21%
Na_2O(eq)	0.52%	-	-
f-CaO	0.9%	-	-
NaO	-	0.16%	-
K_2O	-	0.87%	-
C	-	1.12%	-
Loss on ignition	1.21%	2.25%	-
Specific surface area(m^2/kg)	341	18650	422

Table 2. Mixture design

Mixtures	Aggregates			Cementitious materials			Relative weight ratio to cementitious materials		
	CS	FS	SS	PI 42.5	SF	GGBS	w/c	s/c	HRWR
SF0	0.2	0.3	0.5	0.45	0.25	0.3	0.2	1	0.02

2.2 Crack generation

A novel splitting device (Fig. 1(a)) was designed to fracture the RPC with a single macro crack, resulting in two perfectly matched halves of plain concrete (Fig. 1(b) and (d)), with fewer fragments flaking off the crack surface. The loading rate was maintained at 0.3 mm/min. The tinfoil block (Fig. 1(c)) was folded to achieve a 0.5 mm width, separating the two surface morphologies by a specific in-between width. To prevent water leakage during permeability testing (Fig. 1(e)), the cracks were laterally sealed with scotch tape. The effective length (w) and depth (L) of the crack were measured at 90 mm and 49.5 mm, respectively.

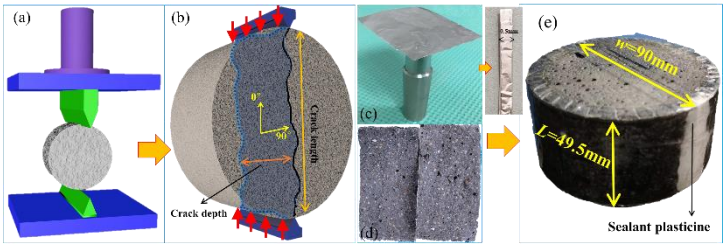

Fig. 1 (a) Self-designed splitting test device, (b) Crack topography in a fully splitted specimen, (c) A sheet of 10 μm tinfoil for 0.5 mm-width block, (d)Top and bottom crack surfaces, (e) Tested specimen for permeability.

2.3 Measurement of permeability, surface width and morphology

Following (Hou et al (2023)), while the flow is in linear, the water permeability test was adopted for the hydraulic parameters including water flow rate (Q) and ∇P, hydraulic width (b_H) can be deduced by Darcy's law, given by $b_H=\sqrt[3]{\frac{12\mu Q}{w\cdot\nabla P}}$, μ are the (Pa·s) denotes the fluid's dynamic viscosity. Bodato digital microscope (magnification =1000×) was used for surface width measurement, recording as b_s, while a laser scanner (ATOS III TRIPLE SCAN, GOM, Germany) digized the surface morphology. Furthermore, the the digital surface morphology and b_s were used for reconstruction of crack topography, note that its sampling interval is 100 μm of re-meshed gridding.

3 Results and discussion

Before healing, the mean crack width (b_M) of the digital crack topography is measured to be 136.79 μm, which is larger than b_s of 123.45 μm. This discrepancy is attributed to the presence of damaged voids and original pores in the concrete crack topography, which prevents the two crack surfaces from perfectly matching. This observation is consistent with a previous study by (Hou et al (2023)). Furthermore, the tested b_H of preconditioned specimens is found to be 54.35 μm, which is smaller than b_M = 136.79 μm. This can be attributed to the fact that interconnected paths alone can facilitate fluid transport, while isolated voids have no contribution to permeability. After healing, it can be observed from Fig. 2(a) that the open mouth of the crack is significantly closed. The closure ratio of the upper and lower surface crack widths are 100% and 95%, respectively. However, it is noted that b_M decreased to 119.47 μm, which is still significantly larger than 0 μm. This can be attributed to the fast closure of the crack near the open mouth, which may have hindered the further sealing process in deeper locations (Fan and Li (2022)). This observation also indicates that the healing process is uneven. In addition, the sealing ratio after healing is found to be 100%, meaning that b_H is reduced to 0 μm. This is due to the fact that the newly formed obstacles have fully closed the interconnected path, as shown in Fig. 2(b). Moreover, the surface roughness coefficient (R_S) decreased from 1.1022 to 1.0938, which can further enrich the feedback model proposed by (Hou et al (2022)). This suggests that the self-healing effect alters the surface roughness, reduces the crack width with obstacles forming in the interconnected paths, and ultimately leads to a decrement in water permeability, potentially even reaching 0.

3. Conclusions

This study suggests that the feedback model in (Hou et al (2022)) between crack topography and water permeability for the self-healing effect can be improved at the ponit where sealing and closure ratios are equal to 1. Results demonstrate that after healing under wet/dry cycles in top water, the crack width

decreases while obstacles increase in the crack topography. These healing products are generated and unevenly distributed within the crack topography, leading to isolated voids even when the water permeability or hydraulic crack width reaches 0, and the interconnected path is fully cut off. Furthermore, our findings indicate that the healing effect also reduces the surface roughness of the crack. Overall, this study sheds light on the complex interplay between crack topography and water permeability during the self-healing process, and provides insights for further research in this field.

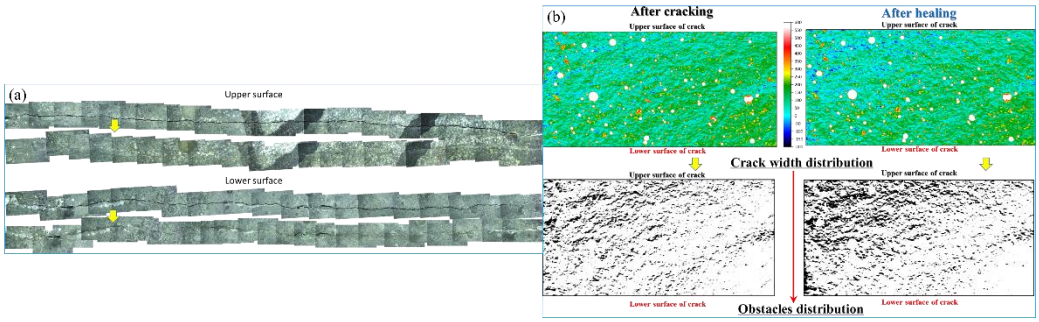

Fig. 2 Pre-conditioning and after-conditioning specimens: (a) Surface crack, (b) Distributions of crack width and obstacles.

Acknowledgements

The authors gratefully acknowledge the financial supports from the Ministry of Science and Technology under Project No. 2018YFC0705400 and the National Natural Science Foundation of China (No. 51908207).

References

Akhavan, A., S.-M.-H. Shafaatian and F. Rajabipour (2012) "Quantifying the effects of crack width, tortuosity, and roughness on water permeability of cracked mortars ". *Cement and Concrete Research*, 42(2): 313-320

Fan, S. and M. Li (2022) "Understanding intrinsic healing process in cementitious cracks through modeling and experiments ". *Cement and Concrete Research*, 162

Hou, S., K. Li, X. Hu and C. Shi (2023) "Influence of crack topography and pressure gradient on nonlinear flow behavior in concrete ". *Cement and Concrete Research*: Under review

Hou, S., K. Li, Z. Wu, F. Li and C. Shi (2022) "Quantitative evaluation on self-healing capacity of cracked concrete by water permeability test – A review ". *Cement and Concrete Composites*, 127: 104404

Huang, H., G. Ye, C. Qian and E. Schlangen (2016) "Self-healing in cementitious materials: Materials, methods and service conditions ". *Materials & Design*, 92: 499-511

Lepech, M. D. and V. C. Li (2009) "Water permeability of engineered cementitious composites ". *Cement and Concrete Composites*, 31(10): 744-753

Mountassir, G. E., R. J. Lunn, H. Moir and E. MacLachlan (2014) "Hydrodynamic coupling in microbially mediated fracture mineralization: Formation of self-organized groundwater flow channels ". *Water Resources Research*, 50(1): 1-16

Suleiman, A. R. and M. L. Nehdi (2018) "Effect of environmental exposure on autogenous self-healing of cracked cement-based materials ". *Cement and Concrete Research*, 111: 197-208

Wu, C., J. Chu, S. Wu and W. Guo (2018) "Quantifying the Permeability Reduction of Biogrouted Rock Fracture ". *Rock Mechanics and Rock Engineering*, 52(3): 947-954

Xiong, F., Q. Jiang, Z. Ye and X. Zhang (2018) "Nonlinear flow behavior through rough-walled rock fractures: The effect of contact area ". *Computers and Geotechnics*, 102: 179-195

Xue, C., M. J. Tapas and V. Sirivivatnanon (2022) "Cracking and stimulated autogenous self-healing on the sustainability of cement-based materials: a review ". *Journal of Sustainable Cement-Based Materials*: 1-23

Yoo, D.-Y., W. Shin, B. Chun and N. Banthia (2020) "Assessment of steel fiber corrosion in self-healed ultra-high-performance fiber-reinforced concrete and its effect on tensile performance ". *Cement and Concrete Research*, 133: 106091

Zhang, W., Q. Zheng, A. Ashour and B. Han (2020) "Self-healing cement concrete composites for resilient infrastructures: A review ". *Composites Part B: Engineering*, 189: 107892